

# EPR DIAGNOSTICS OF DEFECT AND IMPURITY DISTRIBUTION HOMOGENEITY IN SEMI-INSULATING 6H-SiC

D.V. SAVCHENKO, E.N. KALABUKHOVA

UDC 537.635, 548.4  
©2009

V.E. Lashkarev Institute of Semiconductor Physics, Nat. Acad. of Sci. of Ukraine  
(45, Nauka Ave., Kyiv 03028, Ukraine)

The homogeneity of the distribution of impurities and defects in a 6H-SiC wafer cut out from a nominally undoped 6H-SiC ingot grown by the physical vapor transport (PVT) method at the Bandgap Technologies Inc. (USA) has been studied making use of the electron paramagnetic resonance (EPR) and photo EPR methods at a frequency of 37 GHz and the temperature  $T = 77$  K. The researches of the EPR and photo EPR spectra of eleven samples cut off from the wafer have shown that the type of conductivity in the nominally undoped 6H-SiC ingot varies from  $p$ - to  $n$ -type along the growth direction, so that only the middle section of the ingot is characterized by a semi-insulating (SI) behavior due to the mutual compensation of donors and acceptors. In the samples cut off from the middle section of the wafer, the photoresponse of donor and acceptor EPR spectra demonstrates a persistent relaxation effect after the photoexcitation has been turned off, which is a typical characteristic of SI materials. Two intrinsic defects in SI 6H-SiC samples have been found and studied. On the basis of spectroscopic and energy characteristics of defects, one of them was associated with a carbon vacancy in the positive charge state,  $V_C^+$ , while the other was attributed to a silicon vacancy in the negative charge state,  $V_{Si}^-$ .

middle of the energy gap, as well as manganese, is used as an impurity that compensates shallow donors and acceptors [1]. As defects that compensate shallow donors and acceptors, growth defects can be used. Such nominally undoped silicon carbide with a concentration of residual impurities of the order of  $10^{15}$   $\text{cm}^{-3}$  is classed to high-purity SI substances. It is characterized by a high resistance (of the order of  $10^{10}$   $\Omega \times \text{cm}$ ) at room temperature.

A number of works were devoted to studying the nature of defect growth in SI silicon carbide by the EPR method [2–10]. They mainly dealt with polytype 4H, whereas only work [11] considered polytype 6H. However, those researches were usually carried out using small specimens, which did not enable one to get an idea of the SI properties of the whole ingot, which the given wafer was cut out from.

This work aimed at studying the uniformity of the defect and impurity distribution in nominally undoped 6H-SiC by applying the electron paramagnetic resonance (EPR) method and the EPR method with photoexcitation (the photo EPR).

## 1. Introduction

In the last decade, large attention has been given to the development of the technology aimed at obtaining silicon carbide (SiC) single crystals with SI properties, which are used as substrates in manufacturing the high-power microwave devices on the basis of SiC and GaN. However, despite that the world industry already produces this substance, its cost is rather high, although the quality is rather poor. Among the origins of those shortcomings is the fact that the distribution of impurities and defects remains inhomogeneous over a SiC ingot with SI properties, and a lot of defects that are formed during the ingot growing are thermally unstable, which can lead to a degradation of devices, if such a material is used as substrates.

One of the methods to produce a SI substance is to introduce impurities or defects with deep levels in the forbidden gap (FG) at the stage of crystal growing. Vanadium, which forms a number of deep levels in the

## 2. Experimental Specimens and Technique

The diagnostics of the impurity and defect distribution uniformity over the nominally undoped substance 6H-SiC was carried out making use of a 6H-SiC wafer. The wafer, in its turn, was cut out from an ingot grown up by the physical vapor transport (PVT) method [12] at the Bandgap Technologies Inc. (USA). The ingot was grown along the [0001] axis. Figure 1 illustrates how a wafer to study was cut out from the ingot. The wafer had a crystallographic plane (11 $\bar{2}$ 0), which allowed the data to be obtained on the uniformity of the impurity and defect distribution in the ingot along the direction of its growth, from the starting to the upper edge.

The  $24.5 \times 44.5 \times 0.35$ -mm<sup>3</sup> wafer was cut into 13 specimens, each about  $1.7 \times 4$  mm<sup>3</sup> in size, designated

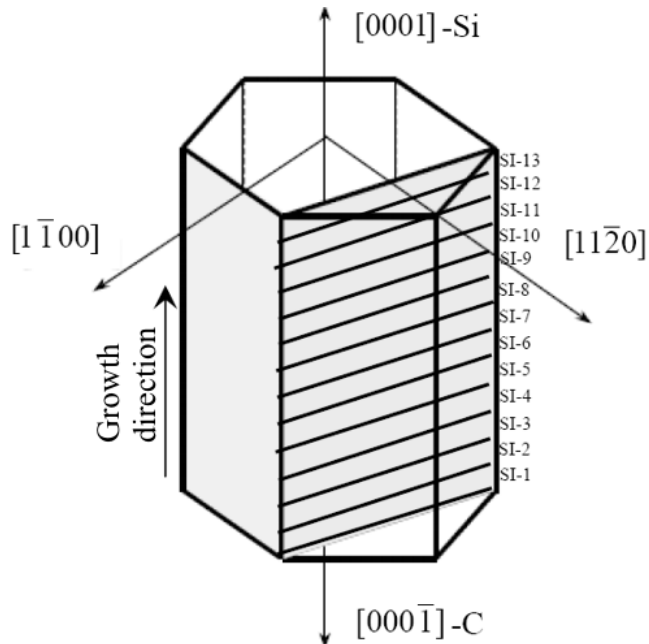


Fig. 1. Schematic of a SI 6H-SiC ingot under investigation

as SI-1 to SI-13. The EPR spectra were studied for 11 specimens. Only two specimens, SI-1 and SI-13 cut out from the opposite ends of the wafer were not researched.

Before carrying out experiments, the specimens were annealed in an inert atmosphere at  $T = 1800$  °C to remove surface defects which are known to be always present in a SI substance before its annealing and characterized by an EPR signal with the isotropic  $g$ -factor:  $g_{\parallel} = g_{\perp} = 2.0025$  [2–5,13].

The spectral measurements by the EPR and photo EPR methods—the latter also includes photoexcitation and photoannealing of the specimens—were carried out on a  $Q$ -Band EPR spectrometer at the temperature  $T = 77$  K.

Specimens were photoexcited by various light sources. Illumination of a specimen with interband ultraviolet light was carried out making use of a 250-W high-pressure mercury vapor lamp in combination with interference filters with wavelengths ranging from 365 to 380 nm. To illuminate a specimen with impurity light, a 100-W xenon and halogen incandescent lamps were used in combination with either an UM-2 prism monochromator or the interference or glass filters, which enabled us to carry out photo EPR experiments in the wavelength range from 380 to 1000 nm. Light focused by a lens was directed to a resonator through an optical fiber. A specimen was mounted on the end face of the fiber and oriented in such a manner that the axis  $c$  of the

crystal was perpendicular to the direction of the external magnetic field  $\mathbf{B}_0$ . To focus light, a biconvex short-focus quartz lens was used.

As a reference specimen at the determination of EPR spectrum parameters, conduction electrons in silicon with  $g = 1.99875 \pm 0.0001$  were used. The EPR spectra were simulated with the help of an Easyspin-2.7.0 module [22]. The line shape was Gaussian. The determination error for the defect and impurity energy levels was approximately  $\pm 0.06$  eV. The determination error of the  $g$ -factor was  $\pm 0.0002$ .

### 3. Experimental Results

The 6H-SiC specimens to study were divided into four groups. The dark EPR spectra for the specimens within each group were identical. The first group included specimen SI-2 only, whose dark spectrum measured at  $T = 77$  K demonstrated very weak EPR signals given by boron, which substituted the quasicubic “K” and hexagonal “T” positions in the 6H-SiC lattice. The second group included specimen SI-3: in its dark EPR spectrum measured at  $T = 77$  K, a contribution of an intrinsic defect was observed. The third group consisted of specimens SI-4 and SI-5: no EPR signal was observed in their EPR spectra in dark. At last, the fourth group of specimens includes specimens from SI-6 to SI-12: in their dark EPR spectra, the EPR spectra of nitrogen which replaced the quasicubic positions in 6H-SiC were observed.

We studied the EPR spectra in all four groups of 6H-SiC specimens both in dark and when photoexciting the specimens by light with various wavelengths. Figure 2 demonstrates that, in specimen SI-2 in dark, there were observed very weak EPR signals with an unresolved hyperfine structure (HFS) from boron  $^{11}\text{B}$  in two quasicubic (“K”)— $\text{B}_{K1}$  and  $\text{B}_{K2}$  ( $g_{\perp} = 2.0045$ )—and one hexagonal (“T”)— $\text{B}_{T}$  ( $g_{\perp} = 2.0068$ )—positions in the 6H-SiC lattice which have  $C_{3V}$ -symmetry at temperatures above 50 K [14]. If specimen SI-2 was photoexcited by interband light, its EPR spectrum revealed signals from two “K” positions of nitrogen  $^{14}\text{N}$ ,  $\text{N}_{K1}$  ( $g_{\perp} = 2.0026$ ) and  $\text{N}_{K2}$  ( $g_{\perp} = 2.0030$ ) [15], which disappeared immediately after the illumination of the specimen by light was ceased.

In Fig. 2-2, the EPR spectrum of specimen SI-3 observed in dark at  $T = 77$  K and  $\mathbf{B}_0 \perp \mathbf{c}$  is depicted (spectrum a). It consists of three single lines designated as XX1, XX2, and XX3, which have axially symmetric  $g$ -factors and isotropic widths, and which correspond to three nonequivalent positions of a defect center in the

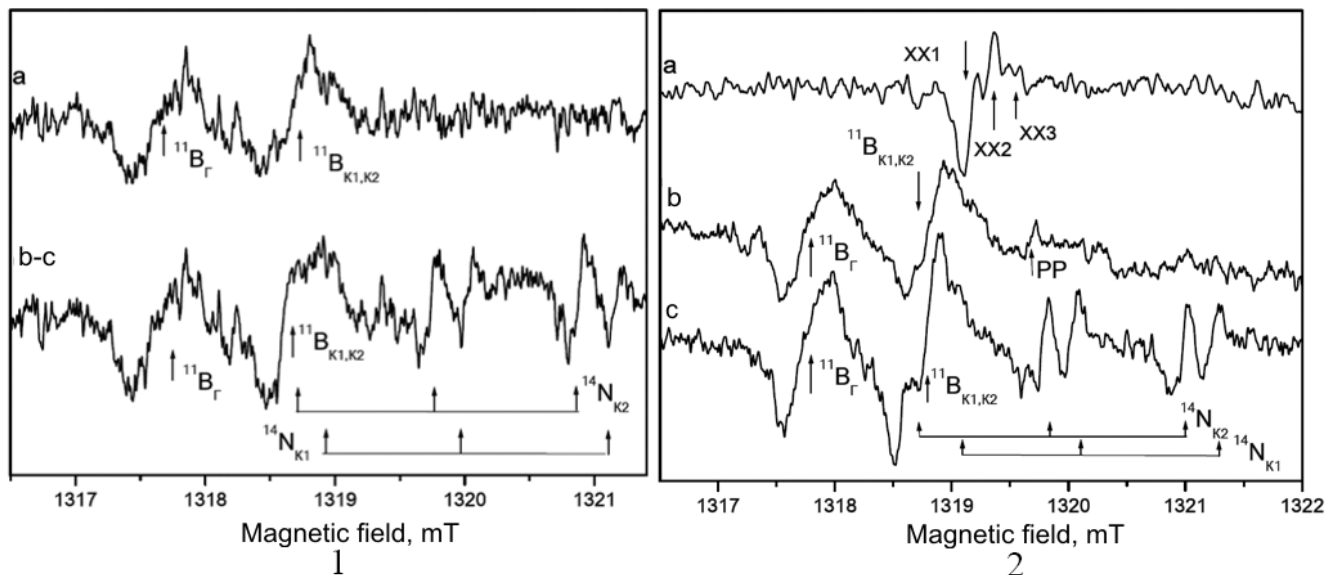


Fig. 2. EPR spectra of SI 6H-SiC specimens SI-2 (1) and SI-3 (2) observed in dark (a) and when the specimens are photoexcited with impurity (b) or interband (c) light.  $\mathbf{B}_0 \perp \mathbf{c}$ ,  $\nu = 37$  GHz, and  $T = 77$  K

6H-SiC lattice. At temperatures below 40 K, the symmetry of EPR spectra  $XX_{K1}$  and  $XX_{K2}$  from the defect that substitutes quasicubic positions in the 6H-SiC lattice becomes lower: it changes from axial to monoclinic one. The parameters of EPR spectra of the observed defect with  $S = 1/2$  and its energy characteristics were obtained in work [11] and are quoted in the Table.

Thus, a unique paramagnetic center, which was observed in dark in specimen SI-3, was defect XX. Hence, its level depth has to determine the position of the Fermi level in the FG of this specimen:  $E_i = \Delta E_{FG} - 1.88$  eV =  $E_V + 1.24$  eV [11], where  $\Delta E_{FG}$  is the width of the forbidden gap in 6H-SiC, and  $E_V$  is the edge of the valence band (VB).

The situation changes drastically, if specimen SI-3 is illuminated with light. In Fig. 2-2, the spectra b and c demonstrate the photoannealing of EPR spectra in specimen SI-3 illuminated with impurity and interband light, respectively. As is seen from this figure, the

photoexcitation of specimen SI-3 with impurity light gives rise to the photoannealing of EPR lines given by XX defect and to the appearance of EPR signals from boron, which substitutes three nonequivalent positions in the 6H-SiC lattice. Those positions were in an ionized state in dark, due to the compensation of their charge state by XX defect.

Simultaneously with the disappearance of EPR signals from XX defect, there appears an EPR signal from the defect center. This signal is designated as PP, and its parameters are quoted in the Table. The notations for defects was selected by analogy with those adopted for two thermally stable intrinsic defects X and P, which are observed in a high-purity SI 4H-SiC and the parameters of which, for the sake of comparison, are also quoted in the Table.

Subsequent illumination of the specimen with interband light leads to an increase of intensity of EPR signals from boron and to the emergence of EPR signals from nitrogen which substitutes quasicubic ( $N_{K1}$  and

**Ionization energies and parameters of EPR spectra of XX and PP defects with  $S = 1/2$  observed in SI 6H-SiC at  $T = 77$  K and their comparison with literature data**

	XX3( $\Gamma$ )	XX2(K)	XX1(K)	PP( $\Gamma$ )	Ky3( $\Gamma$ )	Ky2(K)	Ky1(K)	$X_\Gamma$	$X_K$	$P_\Gamma$	$P_K$
$g_{\parallel}$	2.0024	2.0027	2.0035	2.0047	2.0025	2.0028	2.0036	2.0025	2.0028	2.0048	2.0037
$g_{\perp}$	2.0045	2.0043	2.0040	2.0028	2.0045	2.0043	2.0041	2.0044	2.0043	2.0030	2.0037
Suggested model	$V_C^+$	$V_C^+$	$V_C^+$	$V_{Si}^-$	$V_C^+$	$V_C^+$	$V_C^+$	$(V_C + H)^{-/0}$	$(V_C + H)^{-/0}$	$V_{Si}^{3-}$	$V_{Si}^{3-}$
$E_i - E_V$ , eB	1.24	1.24	1.24	1.29	—	—	—	1.90	2.00	2.10	2.10
Polytype	6H	6H	6H	6H	6H	6H	6H	4H	4H	4H	4H
Source					[17]	[17]	[17]	[18]	[18]	[5]	[5]

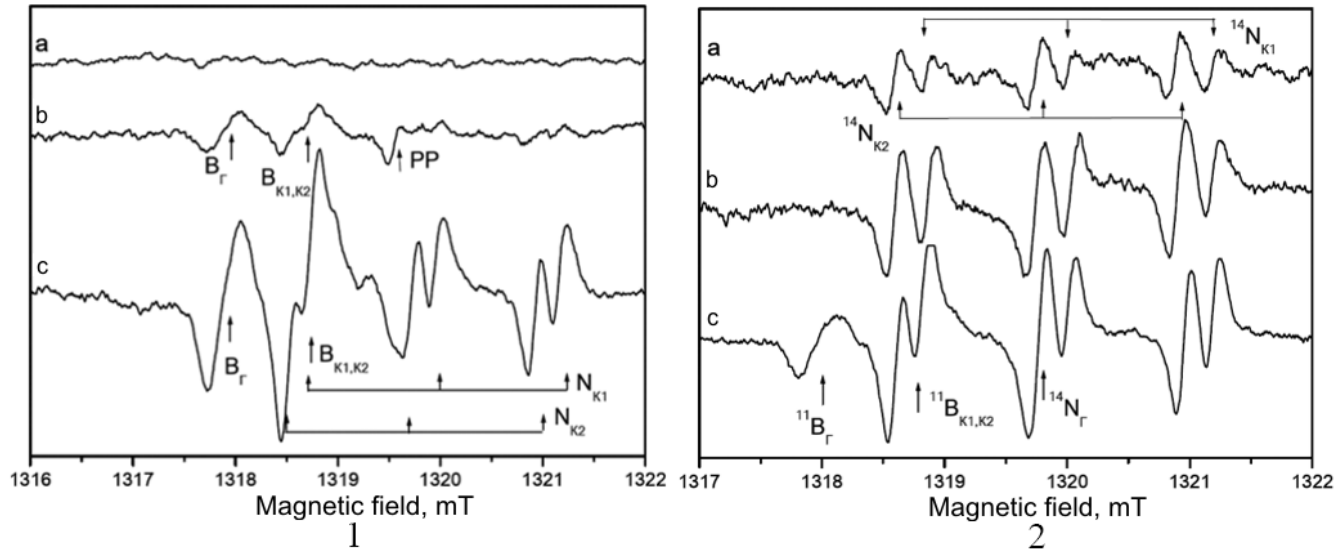


Fig. 3. EPR spectra in the SI 6H-SiC specimens of the third (specimens SI-4 and SI-5) (1) and the fourth (specimens SI-6 to SI-12) (2) groups observed at  $T = 77$  K in dark (a) and when the specimens are photoexcited with impurity (b) or interband (c) light.  $\mathbf{B}_0 \perp \mathbf{c}$  and  $\nu = 37$  GHz

$N_{K2}$ ) positions in the 6H-SiC lattice. After the photoexcitation was terminated, the photo EPR spectra of nitrogen and boron demonstrate a persistent relaxation of their photoresponse.

As shown in Fig. 3, no EPR signal in dark was observed in the third group of specimens (SI-4 and SI-5). If specimen SI-4 was illuminated with impurity light characterized by the photon energy  $h\nu = 1.24 - 1.29$  eV, an EPR signal from PP defect appeared in the EPR spectrum, which gave the basis to estimate the energy level of PP defect in the forbidden gap of 6H-SiC:  $E_i = \Delta E_{FG} - 1.88$  eV =  $E_V + 1.29$  eV [11]. Therefore, it turned out that PP and XX defects have close values of energy levels in the FG.

As is seen from the Table, PP and XX defects have different signs of the  $g$ -tensor anisotropy. In view of the fact that the signs of the  $g$ -tensor anisotropy are different for donors and acceptors in silicon carbide [20], we may suppose that the energy level of PP center, for which  $g_{\parallel} > g_{\perp}$ , has to be closer to the bottom of the conduction band (CB) than the energy level of XX center.

Illumination of specimens SI-4 and SI-5 with interband light leads to the photoannealing of the EPR signal given by PP defect and to the emergence of a signal from nitrogen in the EPR spectrum. The intensity of EPR signals from boron becomes several times stronger at that. After the photoexcitation termination, the photo EPR signals from nitrogen and boron in specimens SI-

4 and SI-5 reveal the persistent relaxation of their photoresponse.

The fourth group, as is seen from Fig. 3-2, contained specimens SI-6 to SI-12, the dark EPR spectra of which revealed EPR signals of nitrogen ( $N_{K1}$  and  $N_{K2}$ ). If the specimens were illuminated with impurity light, the intensity of EPR signals from nitrogen became 1.9 times larger. The following illumination of specimens with interband light gave rise to the subsequent growth of intensity of EPR signals from nitrogen and to the appearance of EPR signals from nitrogen ( $N_{\Gamma}$ ) and boron ( $B_{\Gamma}$ ), which substitute "Γ"-position in the 6H-SiC lattice. However, after the photoexcitation termination, the EPR spectra of nitrogen and boron in specimens SI-6 to SI-12 did not demonstrate the persistent relaxation of the photoresponse.

Hence, a series of photosensitive paramagnetic centers were observed in all four groups of semi-insulating 6H-SiC specimens that were cut off from the same wafer. Those centers can be activated into a paramagnetic or a nonparamagnetic state by photoexcitation. Two of them are the well-known nitrogen and boron impurities, the other two are intrinsic defects with deep levels in the FG.

#### 4. Discussion of Results

A comparison of the parameters obtained for the  $g$ -tensors of EPR spectra of XX defect with the literature

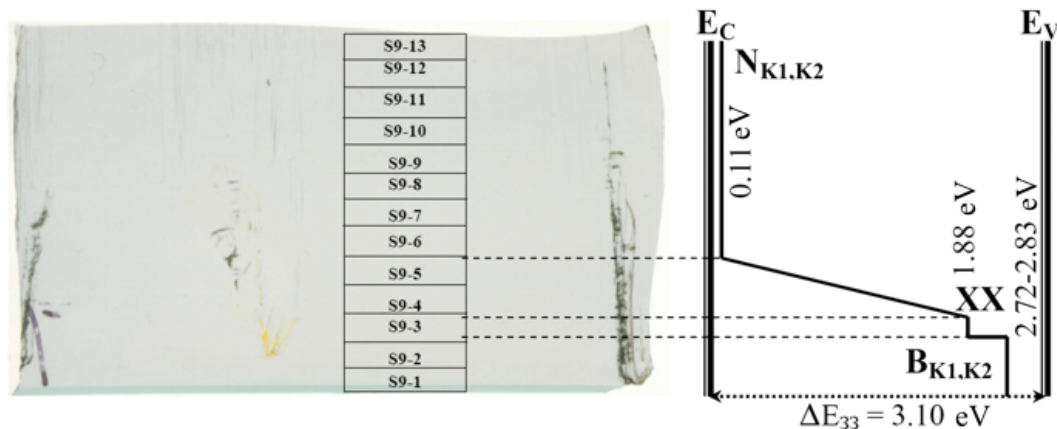


Fig. 4. External view of the studied SI 6H-SiC wafer in the  $11\bar{2}0$  plane (on the left) and the position of the Fermi level along this wafer, which is determined by the energy level of impurity or defect, the EPR spectrum of which is observed in dark (on the right)

data (see the Table) testifies that the parameters of the  $g$ -tensors of XX defect and their temperature behavior coincide with the parameters of the  $g$ -tensors of X defect, which is observed in a high-purity SI 4H-SiC, and the radiation-induced Ky defect, which was observed in the 6H-SiC of the  $p$ -type. The study of the ligand structure of Ky defect allowed it to be classed as a carbon vacancy in a positively charged state,  $V_C^+$  [17]. Therefore, the coincidence of the EPR spectrum parameters of XX defect with the corresponding values for X and Ky defects allowed a conclusion to be made that the XX defect also belongs to carbon vacancies. The fact that the XX defect level is located in the lower part of the FG (see the Table) evidences for its acceptor character. Hence, similarly to the radiation-induced Ky defect, it can be classed as a carbon vacancy in a positively charged state,  $V_C^+$ .

A comparison of the parameters of EPR spectra of PP and P defects (P defect substitutes a hexagonal position in a high-purity SI 4H-SiC) testifies that they are close to each other. On the basis of the analysis of the ligand structure of P defect, the latter was classed as a silicon vacancy in the  $3^-$  charged state,  $3: V_{Si}^{3-}$  [5]. It allowed us to make an assumption that PP defect also belongs to silicon vacancies, the charged state of which is determined by the defect level depth in the FG.

Bearing in mind that the level depth of PP defect agrees well with the value theoretically calculated in works [16, 19] for a silicon vacancy in the negative charged state  $0/-$  (by 1.28 eV above the valence band in 4H-SiC), a conclusion can be drawn that PP defect is a silicon vacancy in the negative charged state  $0/-$  ( $V_{Si}^-$ ). Unfortunately, there are no reliable data in the

literature concerning the parameters of EPR spectra of silicon vacancy in the  $0/-$  ( $V_{Si}^-$ ) charged state in 6H-SiC [21].

## 5. Conclusions

The study of EPR spectra of ten silicon carbide specimens, which a wafer cut out from a nominally undoped 6H-SiC ingot was cut into, has shown that the distribution of defects and impurities in the wafer and, hence, in the ingot is non-uniform. Since the position of the Fermi level in specimens is governed by the level depth of impurity or defect, the EPR spectrum of which is observed in dark, a conclusion can be drawn that it is different in four groups of specimens.

In Fig. 4, the external view of a SI 6H-SiC wafer is shown, as well as the illustration of how the position of the Fermi level changes along the wafer, i.e. in the direction of ingot growth (from the external to the starting edge).

In the specimens cut off from that part of the wafer which corresponded to the starting section (specimen SI-2), the position of the Fermi level was determined by the energy level of boron acceptors with the energy level  $E_i = E_V + 0.3$  eV in the FG of 6H-SiC [20]. In the next layer (specimen SI-3), the position of the Fermi level was determined by the energy level of XX defect with the energy level  $E_i = E_V + 1.24$  eV in the FG. In the middle part of the wafer (specimens SI-4 and SI-5), the Fermi level was located above the level of XX defect. In addition, the persistent relaxation of the photoresponse of donor and acceptor EPR spectra was observed in specimens SI-3 to SI-5 after

the photoexcitation termination, which is characteristic of a substance with SI properties. In the part of the wafer that corresponded to the ingot edge opposite to the starting one (specimens SI-6 to SI-12), the position of the Fermi level was determined by the energy level of nitrogen which substituted the quasicubic positions in 6H-SiC and located in the FG at  $E_i = E_C - (0.142 \div 0.137)$  eV [20],  $E_C$  being the conduction band edge.

Thus, we may conclude that, in a nominally undoped 6H-SiC ingot grown up by the physical vapor transport method, the type of conductivity changes from  $p$ - to  $n$ -type along the direction of ingot growth, and that the middle part of the ingot owing to the mutual compensation of shallow donors and acceptors has SI properties. This means that only the wafers cut out from the middle part of the ingot in the crystallographic plane (0001) are characterized by SI properties, whereas the wafers cut out from the starting or the end edge have the conductivity of  $p$ - or  $n$ -type, respectively.

The authors express their gratitude to S.M. Lukin and V. Mitchell for useful discussions. We are also grateful to T.S. Sadarshan and Yu.I. Khlebnikov for providing us with a 6H-SiC wafer to study.

1. M. Bickermann, D. Hofmann, T.L. Straubinger *et al.*, Appl. Surf. Sci. **184**, 84 (2001).
2. E.N. Kalabukhova, S.N. Lukin, A. Saxler, W.C. Mitchel *et al.*, Phys. Rev. B **64**, 235202 (2001).
3. E.N. Kalabukhova, S.N. Lukin, W.C. Mitchel *et al.*, Physica B **308-310**, 698 (2001).
4. E.N. Kalabukhova, S.N. Lukin, D.V. Savchenko, W.C. Mitchel, and W.D. Mitchel, Mat. Sci. Forum **457-460**, 501 (2004).
5. E.N. Kalabukhova, S.N. Lukin, D.V. Savchenko, and W.C. Mitchel, Physica B **340-342**, 156 (2003).
6. V.V. Konovalov, M.E. Zvanut, and J. van Tol, Phys. Rev. B **68**, 012102 (2003).
7. W.E. Carlos, E.R. Glaser, and B.V. Shanabrook, Mat. Sci. Forum **457-460**, 457 (2004).
8. N.T. Son, B. Magnusson, Z. Zolnai, A. Ellison, and E. Janzen, Mat. Sci. Forum **433-436**, 45 (2003).
9. N.T. Son, B. Magnusson, Z. Zolnai, A. Ellison, and E. Janzen, Mat. Sci. Forum **457-460**, 437 (2004).
10. N.T. Son, P. Carlsson, B. Magnusson, and E. Janzen, Mat. Sci. Forum **556-557**, 465 (2007).
11. D.V. Savchenko, E.N. Kalabukhova, S.N. Lukin *et al.*, Mat. Res. Soc. Symp. Proc. **911**, B05-07 (2006).
12. D.W. Snyder, V.D. Heydemann, W.J. Everson, and D.L. Barrett, Mat. Sci. Forum **338-342**, 9 (2000).
13. P.J. Macfarlane and M.E. Zvanut, Vac. Technol. B **17**, 1627 (1999).
14. S. Greulich-Weber, F. Feege, E.N. Kalabukhova *et al.*, Semicond. Sci. Technol. **13**, 59 (1998).
15. S. Greulich-Weber, M. Feege, J.-M. Spaeth, E.N. Kalabukhova *et al.*, Solid State Commun. **93**, 393 (1995).
16. A. Zywiets, J. Furthmuller, and F. Bechstedt, Phys. Rev. B **59**, 15166 (1999).
17. V.Ya. Bratus, T.T. Petrenko, S.M. Okulov, and T.L. Petrenko, Phys. Rev. B **71**, 1252026 (2005).
18. E.N. Kalabukhova, S.N. Lukin, D.V. Savchenko *et al.*, Mat. Sci. Forum **527-529**, 559 (2006).
19. L. Torpo, M. Marlo, T.E.M. Staab, and R.M. Nieminen, J. Phys.: Condens. Matter. **13**, 6203 (2001).
20. S. Greulich-Weber, Phys. Status Solidi A **162**, 95 (1997).
21. N.T. Son, M. Wagner, C.G. Hemmingsson, L. Storasta, B. Magnusson, W.M. Chen, S. Greulich-Weber, J.-M. Spaeth, and E. Janzén, in *Silicon Carbide, Recent Major Advances*, edited by W.J. Choyke, H. Matsunami, and G. Pensel (Springer, Berlin, 2004), p. 461.
22. S. Stoll and A. Schweiger, J. Magn. Reson. **177**, 390 (2005).

Received 28.11.08.

Translated from Ukrainian by O.I. Voitenko

#### ЕПР-ДІАГНОСТИКА ОДНОРІДНОСТІ РОЗПОДІЛУ ДЕФЕКТІВ ТА ДОМІШОК У НАПІВІЗОЛЮЮЧОМУ 6H SiC

Д.В. Савченко, К.М. Калабухова

#### Резюме

У роботі представлено результати діагностики методом електронного парамагнітного резонансу (ЕПР) та фото-ЕПР на частоті 37 ГГц при  $T = 77$  К однорідності розподілу дефектів та домішок у пластині 6H SiC, вирізаній із спеціально нелегованого 6H SiC злитка, вирощеного газотранспортним методом на фірмі Vandgar Technologies Inc. (США). Дослідження спектрів ЕПР та фото-ЕПР одинадцяти зразків 6H SiC, на які було розрізано пластину, показало, що у спеціально нелегованому злитку 6H SiC тип провідності змінюється вздовж напрямку росту злитка від  $p$ - до  $n$ -типу, і тільки його середня частина, завдяки взаємній компенсації мілких донорів та акцепторів, виявляє напівізолюючі (НІ) властивості. У зразках, відрізанних від середньої частини пластини, спостерігалось явище довготривалої релаксації фотовідгуку після припинення фотозбудження, яке є характерною ознакою матеріалу з НІ-властивостями. Виявлено та вивчено спектри ЕПР та фото-ЕПР двох власних дефектів у зразках, що мають напівізолюючі властивості. На основі отриманих спектроскопічних та енергетичних характеристик дефектів зроблено припущення, що один з них відноситься до вуглецевої вакансії у позитивному зарядовому стані  $V_C^+$ , а другий – до вакансії кремнію у негативному зарядовому стані  $V_{Si}^-$ .